Tribology and Materials
Vol. 2, No. 4, 2023, pp. 154-161

ISSN 2812-9717
https://doi.org/10.46793/tribomat.2023.018

Effect of graphene nanoplates on the mechanical and corrosion properties of aluminium nanocomposite fabricated by powder metallurgy

Vivek SHARMA, Ashis MALLICK *, Kartikay KUMAR

Department of Mechanical Engineering, Indian Institute of Technology (Indian School of Mines), Dhanbad, India
*Corresponding author: mallick@iitism.ac.in

Keywords
aluminium
nanocomposite
powder metallurgy
mechanical properties
corrosion

History
Received: 14-09-2023
Revised: 01-11-2023
Accepted: 06-11-2023

Abstract

The focus of the present work is to develop an aluminium metal matrix nanocomposite reinforced with graphene nanoplates (GNP). This study examines the effect of adding a small quantity of GNP on the mechanical properties and corrosion behaviour of the composites. The powder metallurgy approach was employed to fabricate a range of Al/GNP composites, and each of these composites was developed using a different proportion of GNP, ranging from 0 to 0.6 wt. %. The XRD line profile investigations of pure Al and composites were performed to identify the presence of GNP in the composites. Physical and mechanical properties, followed by corrosion resistance, are examined. Micro Vickers hardness and a compression test were conducted to determine the mechanical properties. The corrosion test of the composites was performed using potentiostat. Experimental results reveal that the composite has a noticeable advantage over pure aluminium in terms of hardness, compressive strength and corrosion resistance.

1. Introduction

Rapid research improvements on Al-based materials for various structural applications have been seen in recent years [1,2]. Therefore, a comprehensive experimental study of these materials is of the utmost importance. The demand for these materials has increased substantially in order to reduce exhaust gas emissions and increase operational efficacy in transportation applications, thereby protecting the environment [3,4]. Aluminium has a low density, high thermal and electrical conductivity and a high damping capacity. However, aluminium lacks the necessary hardness and corrosion resistance for most industrial applications.

In order to improve the mechanical and corrosion properties of aluminium-based materials, many studies have focused on the development of alloys and nanocomposites with the aluminium matrix reinforced with hard nanoparticles [5-7]. A thorough investigation of the impact of laser shock peening without coating on the corrosion behaviour of the alloy AA6082-T651 in a close to natural chloride environment was presented by Trdan and Grum [8]. The microstructural characteristics and corrosion resistance of a 6082-T651 aluminium alloy substrate were subsequently examined by Ravnikar et al. [9] in the presence of laser-alloyed TiB_2/TiC/Al composite coatings. Very recently, Dinesh Kumar et al. [10] have studied the effect of ZrB_2 on the microstructure, mechanical and corrosion behaviour of an aluminium alloy matrix composite fabricated by stir casting. Their study showed that the inclusion of micron-sized ZrB_2 into the Al matrix enhanced hardness, ultimate tensile strength and corrosion resistance.

Aluminium matrix composites (AMCs) are one of the leading researched engineering materials due to their appealing features for a wide range of industrial applications. It is considered that

nanoparticles are preferred reinforcement over micron-sized particles for improving mechanical properties in metal matrix composites due to their intrinsic ability to reduce stress concentration at particle-matrix interfaces. The tensile strength of an Al composite reinforced with 1 vol. % Si_3N_4 nanoparticles (approx. 10 nm) is almost identical to that of 15 vol. % SiC micron-sized (3.5 μm) particles, as reported by Ma et al. [11].

Graphene, on the other hand, has grown in popularity as a reinforcing element due to its excellent mechanical and corrosion properties. This low-density two-dimensional carbon family member exhibits good load-bearing capacity when compared to other effective forms of carbon, such as CNTs [8]. Numerous studies have been conducted recently to develop graphene-reinforced nanocomposites. Lava Kumar et al. [12] presented a comprehensive and critical evaluation as well as state-of-the-art research activities on the processing, characteristics and applications of aluminium-graphene nanocomposites. In their review, they emphasised the need for Al-based lightweight metallic materials and the impact of graphene-based nanomaterials as reinforcement on the structure and characteristics of the produced Al matrix nanocomposites. Because of its high interfacial interaction with the matrix material, GNP is one of the most extensively utilised graphite derivatives as reinforcement with diverse matrix combinations [13]. However, one of the major drawbacks is that GNP tends to agglomerate because of their high surface energy, which can reduce the mechanical properties of the composites. Thus, correct fabrication techniques are crucial in order to improve the mechanical and physical properties of the composites.

The open literature search suggests that only a few research have addressed the aluminium nanocomposites reinforced by graphene nanoplates. Among those few research, one studied Al/GNP nanocomposites prepared by powder metallurgy and subsequently processed by a multi-pass drawing at room temperature [14]. The microstructure evolution during the drawing process and the strengthening effects of GNP on Al/GNP composites both before and after the drawing process are included in the analysis of the study. Recently, the thermal characteristics of aluminium composites reinforced with varying wt. % of GNP (less than 2 wt. %) have been predicted using finite element analysis, experimental study and theoretical models [15].

A large number of fabrication methods, such as casting, powder metallurgy (PM), disintegrating melting processes (DMD) and additive manufacturing (AM), can be found for the development of Al-based metal matrix composites [16,17]. In contrast to other fabrication processes, the powder metallurgy method requires low temperatures to fabricate metal matrix composites. As a result, at lower temperatures manufacturing process, the detrimental interfacial reaction between the Al matrix and the reinforcement is forbidden, particularly for carbon-based reinforcements. Additionally, compared to the others, PM shows a more uniform distribution of reinforcement across the matrix [18].

The current study focuses on the development of aluminium metal matrix nanocomposites fabricated by reinforcing with GNP the Al matrix using the powder metallurgy technique. To study the mechanical and corrosion behaviour of the bulk nanocomposites containing different weight percentages of GNP, the microhardness, compression tests at constant strain rates and corrosion tests by using potentiodynamic polarisation were carried out at room temperature. The results revealed that the presence of nanoreinforcement (GNP particles) and their quantity substantially impact the strength and corrosion resistance of bulk nanocomposite samples.

2. Experimental procedures

2.1 Materials and production process

In this work, commercial 99.9 % pure Al powder with a granular size range of 7 to 15 μm was acquired from Alfa Aesar, and GNP with a width of approx. 5 μm and a thickness range of 2 to 10 nm were supplied by ACS Material. Al was chosen as the matrix material, while GNP with various wt. % (0.2, 0.3, 0.4, 0.5 and 0.6) were employed as reinforcement. For homogeneous mixing, the powders of different weight combinations were mixed separately for one hour in a mechanical alloying machine operating run at 300 rpm without the use of balls or a process control agent. The mixture of Al and GNP was cold compacted in a die at a pressure of 500 MPa (approx. 2.56 ton-force) and then sintered at 550 °C for 3 hours in an argon furnace to produce 8 mm diameter and 8 mm length bulk cylindrical composite samples. Figure 1 depicts a schematic illustration of the fabrication

process of Al/GNP nanocomposites. The bulk pure Al sample was fabricated separately from the Al powder using the same process parameters for comparison purposes.

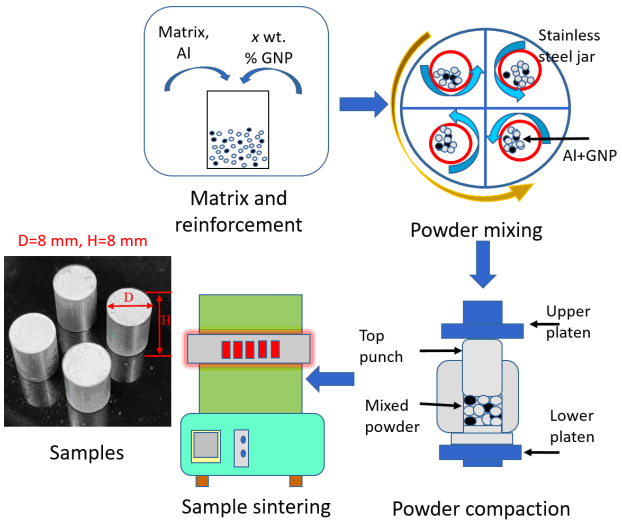

Figure 1. Flowchart of the processing route of Al/GNP nanocomposite using powder metallurgy (PM) method

2.2 Characterisation

The phase information of bulk samples of pure Al and its composites was examined using an X-ray diffractometer (Smartlab, Rigaku). The samples were scanned at a rate of 4 °/min while being subjected to CuKα radiation (λ = 1.54056 Å). Al, graphene and other associated phases were detected by comparing their Bragg angles to their standard values. The morphology of Al powder and GNP was examined using a field emission scanning electron microscope (FESEM) (Supra 55, Carl Zeiss).

The density of the extruded samples was determined experimentally via Archimedes' principle [16] according to ASTM B962. In contrast, the rule-of-mixture was employed to compute the theoretical density of the extruded samples for each composition, taking into account the densities of Al approx. 2.3 g/cm^3 and GNP approx. 2.7 g/cm^3. The tests were repeated at least five times for three samples of each composition.

Compression tests at room temperature were conducted at a constant strain rate of 2×10^{-3} s^{-1} in accordance with the ASTM E9 standard on cylindrical specimens of each composition having 8 mm diameter and 8 mm length. The tests were performed in an H50KS universal testing machine supplied by Hounsfield with a load cell of 25 kN and a sensitivity of 5 N. Prior to testing, the samples were polished and made flat at both ends to avoid surface affliction and sharp edges. In order to get reliable results, three samples of each composition were tested under identical testing conditions.

The microhardness of the bulk composites and pure Al were measured using a fully automatic Micro Vickers hardness tester (supplied by Metco India Ltd.). A static load of 5 N with a dwell time of 30 seconds was applied to the mirror-polished flat surface of the samples using a Vickers pyramid diamond indenter with a face angle of 136°. The average diagonal dimension (d_{ave} = (d_1 + d_2) /2) of the resulting indentation was optically measured and then the hardness in kgf/mm^2 was estimated using the following relationship

$$HV = \frac{0.1891F}{d_{ave}^2}, \quad (1)$$

where F is the load in N, applied to the indenter and d_{ave} is measured in mm. The representative microhardness values of each sample were calculated using the mean value of at least 10 experiments conducted in different locations under the same test conditions.

Corrosion tests on pure Al and Al/GNP composites were carried out using a computer-controlled K-Lyte 1.2 potentiostat (supplied by Kanopy Techno Solutions Pvt. Ltd., India). The tests were performed at room temperature in a 3.5 % NaCl aqueous solution (pH = 7 ± 0.2). To produce an electrode, 5 mm diameter and 5 mm height cylindrical samples of each composition were metallographically polished and then ultrasonically cleaned for 10 minutes. The samples were immersed in a NaCl solution with a surface area of one cm^2 (≈ πr^2 + 2πrh). The corrosion behaviour of the samples was determined using Tafel extrapolation of linear potentiodynamic polarisation (LPP). In this study, Ag/AgCl was used as the reference electrode, while the counter electrode was platinum wire mesh. To ensure the stability of the data, the open circuit potential (OCP) was measured 3 hours after the samples were immersed in the 3.5 % NaCl solution. In order to ensure the consistency of the experimental findings, the electrochemical tests were repeated three times.

3. Results and discussions

The PM method was successfully used to fabricate the bulk samples of pure Al and Al/GNP nanocomposites that contained GNP in five various weight percentages (0.2, 0.3, 0.4, 0.5 and 0.6 wt. %).

3.1 Microstructures

The FESEM images in Figure 2 depict the morphologies of Al powders and GNP. The average dimension of the irregular Al particles was estimated to be 10 µm and the graphene sheets were found to be ultrathin and wrinkly multilayer platelets which are very transparent to the electron beam.

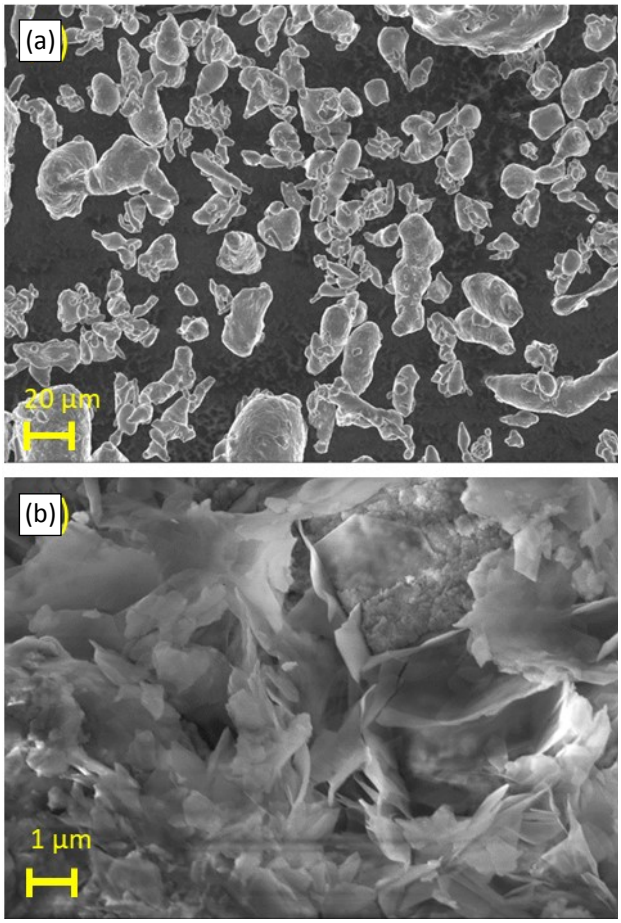

Figure 2. FESEM image of: (a) irregular aluminium particles and (b) graphene platelets

The X-ray diffraction (XRD) patterns of bulk sintered samples of Al and Al/GNP nanocomposites are shown in Figure 3. The XRD result suggests that all of the extruded samples have an Al dominant phase, which corresponds to the crystallographic planes for Al by the peaks of (111), (200), (220) and (311). The (002) peak, corresponding to GNP is not clearly apparent in the full continuous XRD spectra of the extruded composite samples. However, in the enlarged XRD spectra of the nanocomposite samples in the 2θ range ~ 21 – 29°, the GNP peak (002) could be seen. Compared to the Al diffraction peaks, the extremely low-intensity peak of GNP in the diffraction pattern can be attributed to the much lower concentration of the GNP phases and their fine size in the bulk nanocomposites. The XRD result also suggests that the GNP could not form a solid solution with the Al matrix.

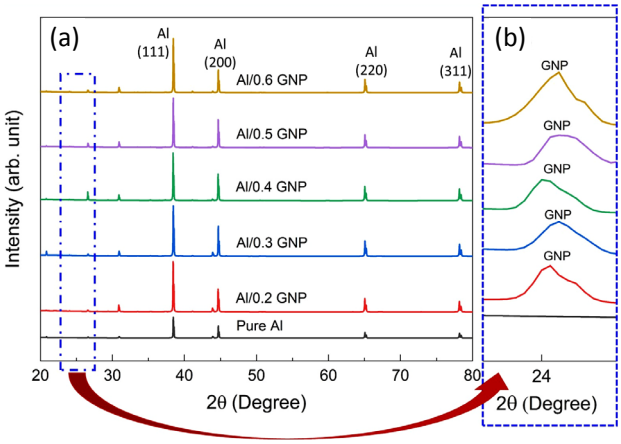

Figure 3. X-ray diffraction (XRD) line profiles of pure Al and Al/GNP composites: (a) full scan and (b) enlarged portion of 2θ ~ 21 to 29°

3.2 Density measurements

As can be seen in Table 1, the argon-sintered bulk pure Al and Al/GNP nanocomposites achieved near theoretical density. As GNP are added progressively, the experimental densities of Al/GNP nanocomposites decrease due to the disparity in density between Al and GNP. Pure Al exhibited a minimum porosity level of approximately 3.09 %. It can be found that the porosity level increased in the composites with the increase of GNP. This may be due to the combined effect of adding a higher volume fraction of GNP reinforcement and the inadequate coupling between the reinforcement and matrix.

Table 1. Density measurement results for fabricated materials

Material	Density, g/cm^3		Porosity, %
	theoretical	experimental	
Pure Al	2.7	2.6165	3.0925
Al/0.2GNP	2.6989	2.6137	3.1568
Al/0.3GNP	2.6984	2.5961	3.7910
Al/0.4GNP	2.6979	2.5747	4.5665
Al/0.5GNP	2.6974	2.5683	4.7860
Al/0.6GNP	2.6960	2.5454	5.9160

3.3 Compression and microindentation analyses

Figure 4 depicts typical engineering stress-strain curves under compressive loading at room

temperature for pure Al and Al nanocomposite samples having varying amounts of GNP as reinforcement. All the stress-strain curves appear to be very similar, with different values of compressive strength and strain to failure. The stress-strain curves revealed that there is a significant improvement in compressive yield strength and ultimate compressive strength in the nanocomposite samples, and the strength increased with the addition of GNP up to 0.4 wt. % only. The composite containing 0.4 wt. % GNP demonstrated the most promising results, and its ultimate compressive strength was increased by approximately 65 % compared to pure Al.

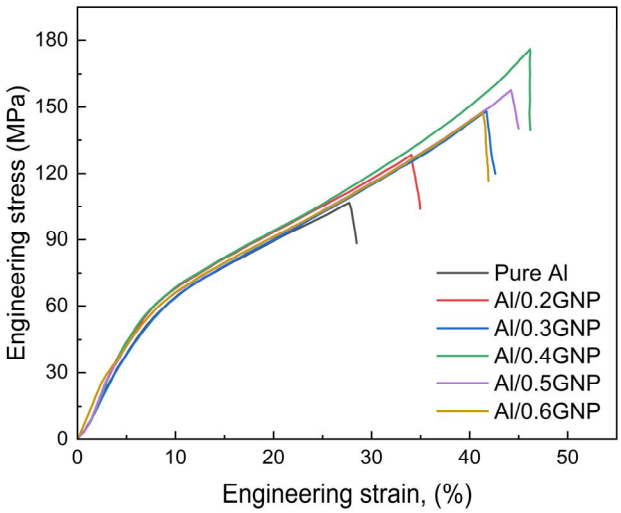

Figure 4. Engineering stress-strain behaviour of pure Al and Al/GNP composites

A number of possibilities, such as the Hall-Petch effect and the even dispersion of nanoreinforcement (2D GNP), contributed to enhancing the compressive strength. Nano-sized GNP efficiently controls grain boundary movements and reduces grain growth in the matrix material. In addition, GNP acts as a barrier to dislocation movement, which contributes to increasing the strength of the composites [18]. Last but not least, a better strengthening effect may be due to the strong bonding of Al and GNP particles and the relatively large surface area of GNP [19]. However, an excess amount of GNP encouraging agglomerations during dispersion in Al matrices may have an adverse effect on grain refining and structural integrity. Thus, the increase in GNP to 0.5 wt. % and above nullified any further increase in strength. The formation of GNP clusters and the formation of a relatively high number of micropores may contribute to lower compressive strengths when GNP levels are higher in the Al matrix.

Figure 5 displays the microindentation-mediated Vickers hardness values for the pure Al matrix sample and Al/GNP composite samples. It is evident that the microhardness of the composites is higher than that of the pure Al sample that was fabricated and tested under identical conditions. Interestingly, after increasing the microhardness values of the composite up to 0.4 wt. % GNP, the further addition of GNP resulted in a drop in the hardness of the Al/GNP composite. The rule of thumb of the dislocation strengthening mechanism is that a larger grain boundary network impedes dislocation motion. Adding GNP to the Al matrix refined the grains and increased the strength of the composite. As previously discussed, the decrease in hardness of composites with 0.5 wt. % or more GNP may be attributable to the irregularities and agglomeration of GNP in the Al matrix. Agglomeration of GNP can lead to graphite, thereby losing its excellent mechanical properties.

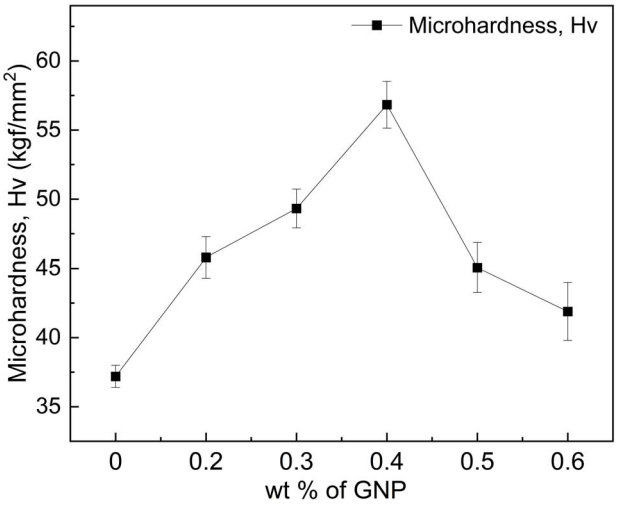

Figure 5. Variation of Vickers microhardness as a function of the concentration of GNP in Al matrix

Table 2 summarises the effect of GNP weight percent in the Al matrix on compressive strength and microindentation hardness. The result suggests a substantial increase in strength upon the addition of 2D GNP as reinforcement; nevertheless, as the quantity of GNP increases, the strength values decrease. The yield strength, compressive strength and hardness gradually increase with an increase in GNP up to 0.4 wt. % and then gradually decrease with an increase in GNP wt. %. It is a fact that there were two obvious variables influencing the strength of the composite: (a) adding a small amount of GNP to the matrix material makes it strengthen as distributed GNP prevents dislocation motions, (b)

Table 2. Effect of GNP concentration in Al matrix on the microhardness and compressive strength

Material	Microhardness HV		Yield strength		Ultimate strength	
	value, kgf/mm²	increase, %	value, MPa	increase, %	value, MPa	increase, %
Pure Al	37.2	–	46	–	106	–
Al/0.2GNP	45.8	23.1	51	10.8	127	19.8
Al/0.3GNP	49.3	32.5	48	4.3	149	40.6
Al/0.4GNP	56.8	52.7	57	23.9	175	65.1
Al/0.5GNP	45.0	21.0	50	8.6	157	48.1
Al/0.6GNP	41.9	12.6	48	4.3	146	37.7

conversely, excessive GNP lowers the mechanical properties due to porosity and nanoparticle clusters, which cause poor bonding between the matrix and the nanoparticles.

3.4 Corrosion behaviour analysis

Figure 6a depicts the open circuit potential (OCP) vs. time curves obtained with pure aluminium and Al/GNP nanocomposites immersed in 3.5 % NaCl solution at room temperature. It is evident that the potential changes over time due to the tendency of surface oxidation to change. The graphs show that after three hours of sample immersion, the electrochemical cell stabilises and no substantial variation can be found in the OCP readings. In order to analyse the corrosion behaviour of the sample, the electrochemical test was conducted after three hours of sample immersion. Figure 6b illustrates the Tafel plots – potentiodynamic polarisation (PP) curves of pure Al and Al/GNP composites in artificial seawater containing 3.5 % NaCl to investigate their corrosion-protective layer.

The electrochemical parameters, including specific values of OCP, corrosion potential (E_{corr}) and corrosion current density on a logarithmic scale (I_{corr}) and at an antilogarithmic scale are presented in Table 3. It can be seen that the current density dropped with the addition of GNP reinforcements. The Al/0.6GNP composite has the lowest corrosion current density of 0.341×10^{-5} A/cm^2 (I_{corr} = – 0.5467 A/cm^2), which is four orders of magnitude lower than the current density of pure aluminium (1.3765×10^{-5} A/cm^2). This finding suggests that adding GNP to the Al matrix enhanced corrosion resistance. It is noteworthy that the corrosion resistance significantly improves with the addition of 0.4 wt. % GNP; subsequent additions of GNP result in only a marginal improvement in corrosion resistance.

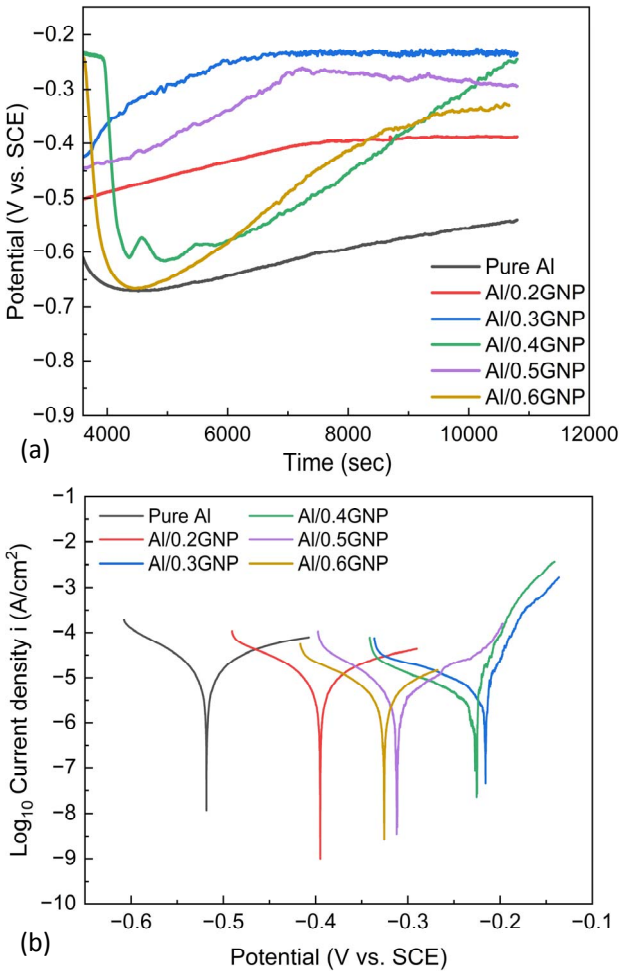

Figure 6. Electrochemical test: (a) open circuit potential (OCP) curves and (b) potentiodynamic polarisation (PP) curves after 10,800 seconds of stabilisation

In order to understand the corrosion behaviour, the corrosion current density was used to calculate the corrosion rate *CR* in mg/cm^2/year using the following relationship [20]:

$$CR = \frac{MT}{F} I_{corr}, \quad (2)$$

where *M* is atomic weight, *F* is the Faraday constant and *T* is the exposure period that converts from year to seconds.

Table 3. Corrosion properties of pure Al and its composite containing from 0.1 to 0.6 wt. % GNP evaluated from electrochemical test

Material	OCP	E_{corr}, V	I_{corr}, A/cm^2	Current density × 10^{-5}, A/cm^2
Pure Al	– 0.540	– 0.5224	– 4.8611	1.3765
Al/0.2GNP	– 0.388	– 0.3982	– 5.0152	0.9669
Al/0.3GNP	– 0.235	– 0.2222	– 5.1864	0.6510
Al/0.4GNP	– 0.244	– 0.2421	– 5.3791	0.4177
Al/0.5GNP	– 0.294	– 0.3053	– 5.4100	0.3990
Al/0.6GNP	– 0.330	– 0.3351	– 5.4671	0.3411

Figure 7 displays the corrosion rates that were obtained from the potentiodynamic polarisation analysis. The results suggest that the composite containing 0.6 wt. % GNP exhibits the least corrosion (10.85 mg/cm^2/year) in simulated seawater, with a 73.19 % improvement in corrosion resistance compared to pure Al (40.48 mg/cm^2/year). This could be explained by the atomic-scale barrier created by the high electron density of GNP, which prevents gas molecules from flowing through the GNP [21].

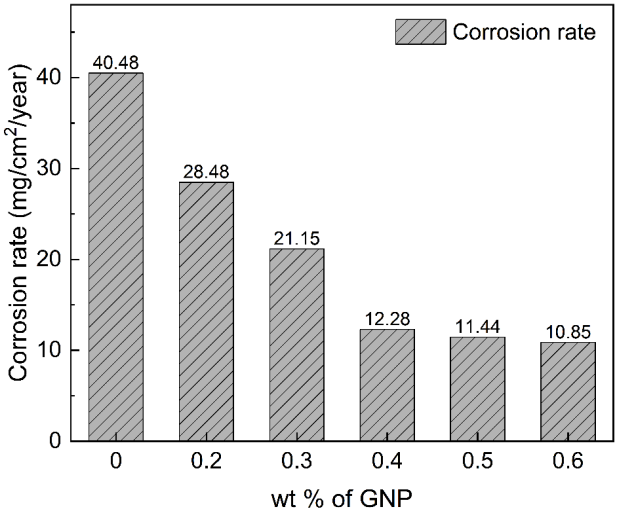

Figure 7. Corrosion rate of Al/GNP nanocomposites obtained from electrochemical polarisation tests

4. Conclusions

Al/GNP nanocomposites containing 0.2, 0.3, 0.4, 0.5 and 0.6 wt. % GNP were successfully synthesised via the PM route in order to achieve high mechanical strength and improved corrosion resistance. FESEM images and XRD analyses were used to characterise the morphology and structure of pure Al and GNP powder and their bulk sintered samples. Mechanical properties and corrosion properties demonstrate that the Al/GNP nanocomposite samples have a significant improvement in compressive strength, microhardness and corrosion resistance when compared to a pure aluminium sample. The nanocomposite containing 0.4 wt. % GNP was found to have the best compressive strength and microhardness among all the fabricated samples. Grain boundary movement, grain boundary diffusion and the geometrically necessary dislocation mechanism may be the possible deformation mechanisms. The present experimental results have great potential for use in the automobile, aerospace, marine and defence industries and can also be extended to the sports and electronics sectors. Due to their lightweight and high specific strength, the present composites can be used to achieve the objectives of environmental sustainability and energy challenges. The mechanical and electrochemical properties obtained in this study can be used to construct a model for the mechanical behaviour and corrosion properties of Al/GNP composites in future studies.

Acknowledgement

The authors wish to acknowledge the research support for this work given by SERB, Department of Science & Technology, Govt. of India, vide Sanction order No. EEQ/2018/001160 dated 18.03.2019.

References

[1] V. Khanna, V. Kumar, S.A. Bansal, Mechanical properties of aluminium-graphene/carbon nanotubes (CNTs) metal matrix composites: Advancement, opportunities and perspective, Materials Research Bulletin, Vol. 138, 2021, Paper 111224, DOI: 10.1016/j.materresbull.2021.111224

[2] K.O. Cooke, Introductory chapter: Structural aluminum alloys and composites, in K.O. Cooke (Ed.), Aluminium Alloys and Composites, IntechOpen, London, 2020, ch. 1, DOI: 10.5772/intechopen.90569

[3] J.C. Benedyk, Aluminum alloys for lightweight automotive structures, in P.K. Mallick (Ed.), Materials, Design and Manufacturing for Lightweight Vehicles, Woodhead Publishing, Cambridge, 2010, pp. 79-113, DOI: 10.1533/9781845697822.1.79

[4] S. Kitipornchai, D. Chen, J. Yang, Free vibration and elastic buckling of functionally graded porous beams reinforced by graphene platelets, Materials & Design, Vol. 116, 2017, pp. 656-665, DOI: 10.1016/j.matdes.2016.12.061

[5] U. Trdan, J. Grum, Evaluation of corrosion resistance of AA6082-T651 aluminium alloy after laser shock peening by means of cyclic polarisation and ElS methods, Corrosion Science, Vol. 59, 2012, pp. 324-333, DOI: 10.1016/j.corsci.2012.03.019

[6] F. Mokdad, D.L. Chen, Z.Y. Liu, D.R. Ni, B.L. Xiao, Z.Y. Ma, Hot deformation and activation energy of a CNT-reinforced aluminum matrix nanocomposite, Materials Science and Engineering A, Vol. 695, 2017, pp. 322-331, DOI: 10.1016/j.msea.2017.04.006

[7] S.O. Akinwamide, B.T. Abe, O.J. Akinribide, B.A. Obadele, P.A. Olubambi, Characterization of microstructure, mechanical properties and corrosion response of aluminium-based composites fabricated via casting – A review, The International Journal of Advanced Manufacturing Technology, Vol. 120, No. 1-2, 2022, pp. 975-991, DOI: 10.1007/s00170-020-05703-1

[8] U. Trdan, J. Grum, SEM/EDS characterization of laser shock peening effect on localized corrosion of Al alloy in a near natural chloride environment, Corrosion Science, Vol. 82, 2014, pp. 328-338, DOI: 10.1016/j.corsci.2014.01.032

[9] D. Ravnikar, R.S. Rajamure, U. Trdan, N.B. Dahotre, J. Grum, Electrochemical and DFT studies of laser-alloyed TiB_2/TiC/Al coatings on aluminium alloy, Corrosion Science, Vol. 136, 2018, pp. 18-27, DOI: 10.1016/j.corsci.2018.02.028

[10] S. Dinesh Kumar, M. Ravichandran, A. Jeevika, B. Stalin, C. Kailasanathan, A. Karthick, Effect of ZrB_2 on microstructural, mechanical and corrosion behaviour of aluminium (AA7178) alloy matrix composite prepared by the stir casting route, Ceramics International, Vol. 47, No. 9, 2021, pp. 12951-12962, DOI: 10.1016/j.ceramint.2021.01.158

[11] Z.Y. Ma, Y.L. Li, Y. Liang, F. Zheng, J. Bi, S.C. Tjong, Nanometric Si_3N_4 particulate-reinforced aluminum composite, Materials Science and Engineering A, Vol. 219, No. 1-2, 1996, pp. 229-231, DOI: 10.1016/S0921-5093(96)10444-5

[12] P. Lava Kumar, A. Lombardi, G. Byczynski, S.V.S. Narayana Murty, B.S. Murty, L. Bichler, Recent advances in aluminium matrix composites reinforced with graphene-based nanomaterial: A critical review, Progress in Materials Science, Vol. 128, 2022, Paper 100948, DOI: 10.1016/j.pmatsci.2022.100948

[13] Z.W. Zhang, Z.Y. Liu, B.L. Xiao, D.R. Ni, Z.Y. Ma, High efficiency dispersal and strengthening of graphene reinforced aluminum alloy composites fabricated by powder metallurgy combined with friction stir processing, Carbon, Vol. 135, 2018, pp. 215-223, DOI: 10.1016/j.carbon.2018.04.029

[14] J. Li, X. Zhang, L. Geng, Improving graphene distribution and mechanical properties of GNP/Al composites by cold drawing, Materials & Design, Vol. 144, 2018, pp. 159-168, DOI: 10.1016/j.matdes.2018.02.024

[15] R. Harichandran, R. Vignesh Kumar, M. Venkateswaran, Experimental and numerical evaluation of thermal conductivity of graphene nanoplatelets reinforced aluminium composites produced by powder metallurgy and hot extrusion technique, Journal of Alloys and Compounds, Vol. 900, 2022, Paper 163401, DOI: 10.1016/j.jallcom.2021.163401

[16] P. Kumar, A. Mallick, M.S. Kujur, K.S. Tun, R. Shabadi, M. Gupta, Strength of Mg-3%Al alloy in presence of graphene nano-platelets as reinforcement, Materials Science and Technology, Vol. 34, No. 9, 2018, pp. 1086-1095, DOI: 10.1080/02670836.2018.1424380

[17] D.B. Miracle, Metal matrix composites – From science to technological significance, Composites Science and Technology, Vol. 65, No. 15-16, 2005, pp. 2526-2540, DOI: 10.1016/j.compscitech.2005.05.027

[18] A. Saboori, M. Pavese, P. Fino, C. Badini, A novel method to homogeneously disperse graphene nanoplateletes in aluminium matrix, in Proceedings of the Euro PM2015, 04-07.10.2015, Reims, France, pp. 1-6.

[19] M.C. Şenel, M. Gürbüz, E. Koç, Mechanical and tribological behaviours of aluminium matrix composites reinforced by graphene nanoplatelets, Materials Science and Technology, Vol. 34, No. 16, 2018, pp. 1980-1989, DOI: 10.1080/02670836.2018.1501839

[20] D.V.P. Tran, P. Sancharoen, P. Klomjit, S. Tangtermsirikul, Effects of concrete mix proportion and chloride content on electrochemical properties of reinforcing steel in concrete, Engineering Journal, Vol. 24, No. 3, 2020, pp. 23-34, DOI: 10.4186/ej.2020.24.3.23

[21] M. Shahin, K. Munir, M. Wen, C. Wen, Y. Li, Microstructure, mechanical and corrosion properties of hot-pressed graphene nanoplatelets-reinforced Mg matrix nanocomposites for biomedical applications, Journal of Alloys and Compounds, Vol. 887, 2021, Paper 161379, DOI: 10.1016/j.jallcom.2021.161379